

Supporting Information for

Diverging Surface Reactions at TiO₂- or ZnO-based Photoanodes in Dye-sensitized Solar Cells

*Raffael Ruess^a, Sabina Scarabino^b, Andreas Ringleb^a, Kazuteru Nonomura^c, Nick
Vlachopoulos^c, Anders Hagfeldt^c, Gunther Wittstock^b and Derck Schlettwein^{a,*}*

- a) Institute of Applied Physics and Center for Materials Research, Justus-Liebig-
University Giessen, Heinrich-Buff-Ring 16, D-35392 Giessen, Germany
- b) Chemistry Department, Carl von Ossietzky University of Oldenburg, D-26111
Oldenburg, Germany
- c) Laboratory of Photomolecular Science, Institute of Chemical Sciences and
Engineering, Swiss Federal Institute of Technology in Lausanne (EPFL), CH-1015
Lausanne, Switzerland.

Evaluation of EIS data

Electron transfer resistance and capacitance at the semiconductor/electrolyte interface

EIS is measured on dye-sensitized solar cells under open-circuit conditions at different background illumination intensities. Typical measurements in Nyquist or Bode (Cole-Cole) representation are shown in Figure S1b and S1c and are fitted with the equivalent circuit depicted in Figure S1a to extract characteristic parameters for the charge-transfer at the semiconductor-electrolyte interface or diffusion of the redox species in the electrolyte.^{1,2} The peak at high frequency can be assigned to the charge-transfer impedance at the semiconductor electrolyte interface.¹ The capacitance of the semiconductor-electrolyte interface C_{se} is plotted logarithmically versus the standard redox potential vs. I_3^-/I^- which was calculated by using the respective standard redox potentials of I_3^-/I^- and $[Co(bpy-pz)_2]^{3+/2+}$ and Nernst's equation. C_{se} usually consist of three different ranges as can be seen in Figure S1d:¹ At positive potentials, the Mott-Schottky capacitance of the blocking layer dominates which appears as an almost constant value in the logarithmic plot. At low potentials, the Helmholtz capacitance of the electrolyte dominates which is barely noticeable but would in general be a constant, limiting capacitance. At intermediate potentials, the chemical capacitance C_μ of the porous semiconductor dominates which is described by equation (SI-1) in which C_0 is a factor describing the amount of interband trap states, α a factor describing the energy distribution of interband trap states, k_B the Boltzmann constant, T the absolute temperature, e the elemental charge, E_{cb} the conduction band edge energy and V_{redox} the redox potential of the electrolyte. For a given V_{oc} between two samples, a vertical shift in the chemical capacitance ($C_{\mu,1}$ vs. $C_{\mu,2}$ in equation (SI-2)) would correspond to a shifted conduction band edge ΔE_{cb} or redox potential ΔV_{redox} , if it is assumed that the samples have a similar total amount and distribution of trap states.¹ Since the redox potential can be calculated by the Nernst equation from the known standard redox potential, the comparison of C_μ will enable an analysis of the relative conduction band positions of samples. This was evaluated for all ED-ZnO and NP-TiO₂ samples in contact to **Co-el** or **I-el** electrolytes and the shift relative to **I-el pure** is shown in Figure 1e.

$$C_\mu = C_0 \exp \left[\frac{\alpha}{k_B T} (eV_{oc} - E_{cb} + eV_{redox}) \right] \quad (SI-1)$$

$$\frac{k_B T}{e\alpha} (\ln C_{\mu,1} - \ln C_{\mu,2}) = \Delta E_{cb} + e\Delta V_{redox} \quad (SI-2)$$

$$V_{ecb} = \Delta V_{oc} - \frac{1}{e} \Delta E_{cb} + \Delta V_{redox} \quad (SI-3)$$

$$R_{rec} = R_0 \exp \left[-\frac{\beta}{k_B T} e V_{ecb} \right] \quad (SI-4)$$

$$\frac{k_B T}{e\beta} (\ln R_{rec,1} - \ln R_{rec,2}) = e\Delta V_{oc}^{rec} \quad (SI-5)$$

The resistance of the semiconductor/electrolyte interface R_{se} , again for all ED-ZnO and NP-TiO₂ samples was plotted logarithmically against the potential V_{ecb} (Figure 1b and d, equation (SI-3)), which is normalized to reference values of V_{redox} and E_{cb} measured in the **pure I-el** electrolyte. An exponential function was fitted to the values at more negative V_{ecb} (Figure S1e), which is characteristic for the recombination resistance R_{rec} in equation (SI-4), in which R_0 is a factor describing the recombination rate independent from energetic alignment and β is a parameter describing the recombination nonlinearity.¹ Since the voltage is corrected by offsets in conduction band energy or redox potential between the DSSCs, the difference in V_{oc} of the cells due to recombination losses ΔV_{oc}^{rec} can be directly compared between two cells ($R_{rec,1}$ vs. $R_{rec,2}$). According to equation (SI-5), ΔV_{oc}^{rec} can be determined as a vertical shift in the recombination resistance at a given V_{ecb} , if it is assumed that the cells have similar short-circuit current density and a similar β . This was evaluated for all ED-ZnO-based and NP-TiO₂-based DSSCs. The voltage loss due to recombination relative to the corresponding sample with **pure I-el** is summarized in Figure 1f. At high voltages recombination can occur via the back layer and result in a decreased slope of R_{se} .¹

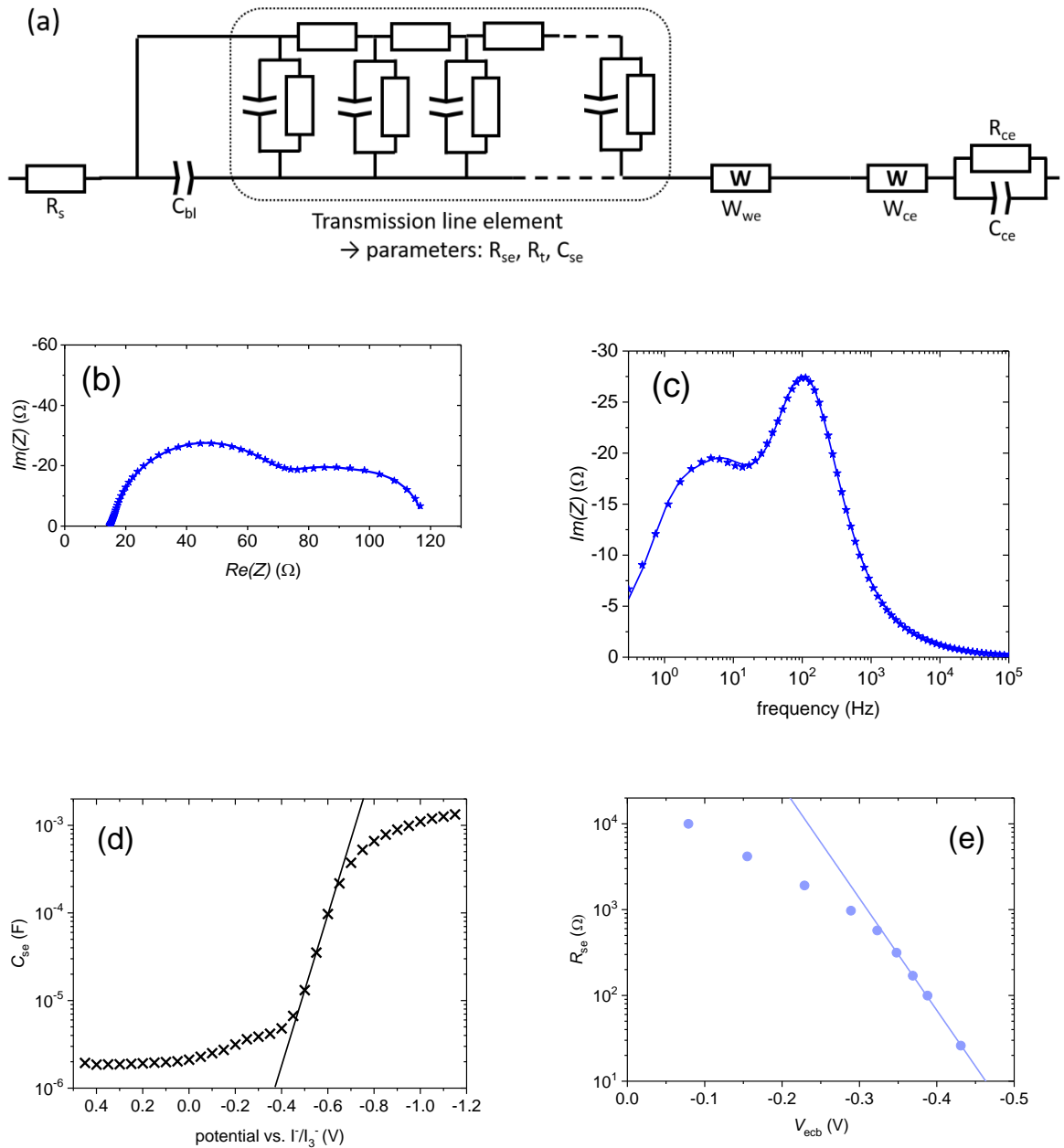
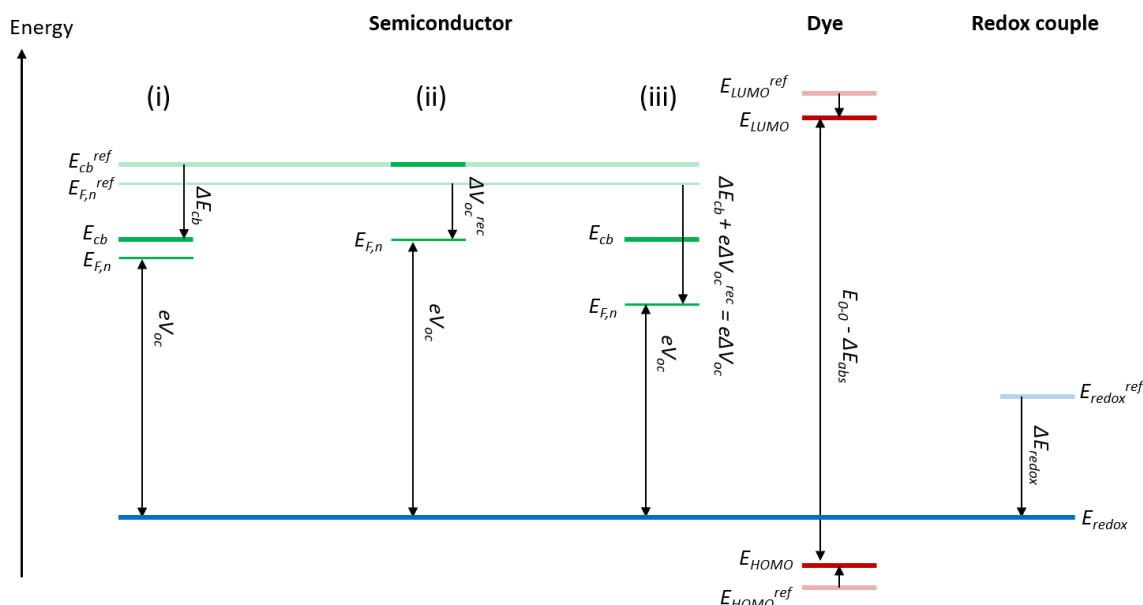


Figure S1. (a) Equivalent circuit for fitting the EIS spectra to obtain the characteristic cell parameters for the charge-transfer at the semiconductor-electrolyte interface or diffusion of the redox species in the electrolyte. EIS measurement data of a ED-ZnO-based DSSC in **Co-el** with **Li⁺** and **TBP** in (b) Nyquist or (c) Bode representation each fitted according to the equivalent circuit (lines). C_{se} of ED-ZnO film measured in aqueous 0.1 M KCl, pH 7, bubbled with N_2 with Ag/AgCl as reference electrode and a Pt wire as auxiliary electrode. (c) R_{se} of a NP-TiO₂ cell with pure **Co-el** electrolyte.



Scheme S1. Schematic energy diagram and open circuit voltage V_{oc} of cells following different modifications of the conduction band edge energy E_{cb} , the relative position of the quasi-Fermi level $E_{F,n}$ or the redox potential E_{redox} of the mediator. A downward shift of E_{cb} (ΔE_{cb}) (i), a higher V_{oc} loss due to faster recombination (ΔV_{oc}^{rec}) leading to a lower $E_{F,n}$ (ii) or the combination of both (iii) cause a variation of V_{oc} . The influence of different E_{redox} (ΔE_{redox}) on V_{oc} and the influence of a Stark shift ΔE_{abs} on the dye energy levels (E_{LUMO} , E_{HOMO} and ground state transition energy E_{0-0}) are also represented. All potentials and energies are referred to reference values shown as transparent lines and denoted as ref , given by the values for ED-ZnO or NP-TiO₂ with the **pure I-I** electrolyte.

Mass transport in the electrolyte

The peak at low frequency in the Bode (Cole-Cole) plots (Figure S1c) can be attributed to the mediator diffusion.¹⁻³ As described in ref.,² a broadening of the right semicircle in the Nyquist plot (Figure S1b) or a broadening of the respective peak in the Bode plot can occur in DSSCs with ED-ZnO photoanodes with cobalt complexes as redox mediator. The impedance spectra have been fitted with the proposed model, where one Warburg impedance element is used to account for diffusion in the porous system and another one for diffusion in the bulk electrolyte.² We note, that two Warburg impedance elements are needed in all cases for the ED-ZnO-based and NP-TiO₂-based DSSCs to achieve a good fit. The Warburg element W_{WE} with high eigenfrequency (low τ_W) is related to diffusion at the porous electrode while the Warburg element W_{CE} with low eigenfrequency (high τ_W) is related to the diffusion at the counter electrode.² It has to be noted that this model is still a rough approximation, since it assumes uniform concentration and diffusion coefficient through the whole porous layer.²

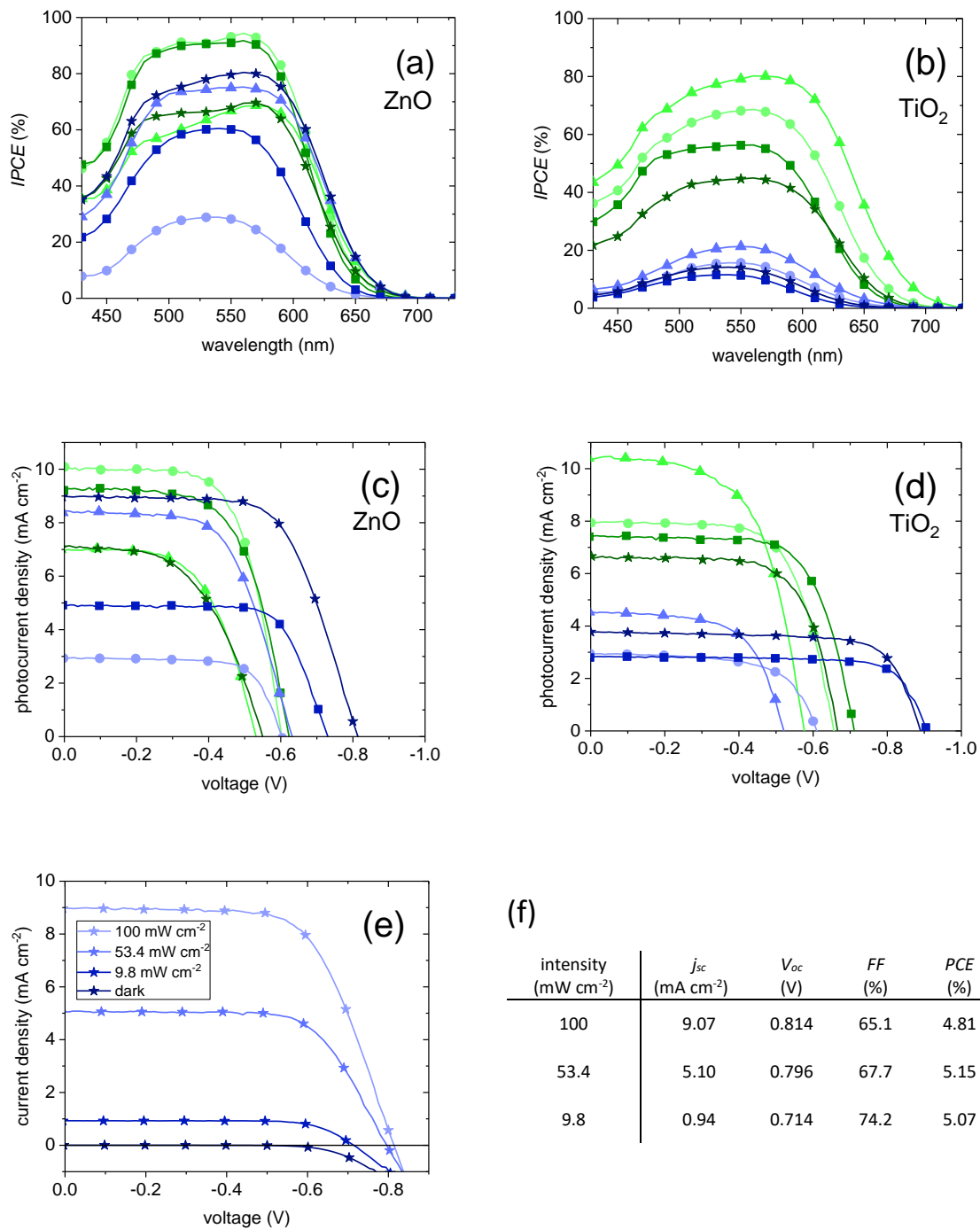


Figure S2. IPCE data of the cells with (a) ED-ZnO or (b) NP-TiO₂ photoanodes and I-V curves of the cells with (c) ED-ZnO or (d) NP-TiO₂ photoanodes in contact to I-el (green symbols) or Co-el (blue symbols), either pure (circles), with Li⁺ (triangles), with TBP (squares) or both Li⁺ and TBP (stars) under standard illumination (100 mW cm⁻²). (e) I-V curves and (f) characteristic parameters of the ED-ZnO-based cell with Co-el with Li⁺ and TBP under different illumination conditions.

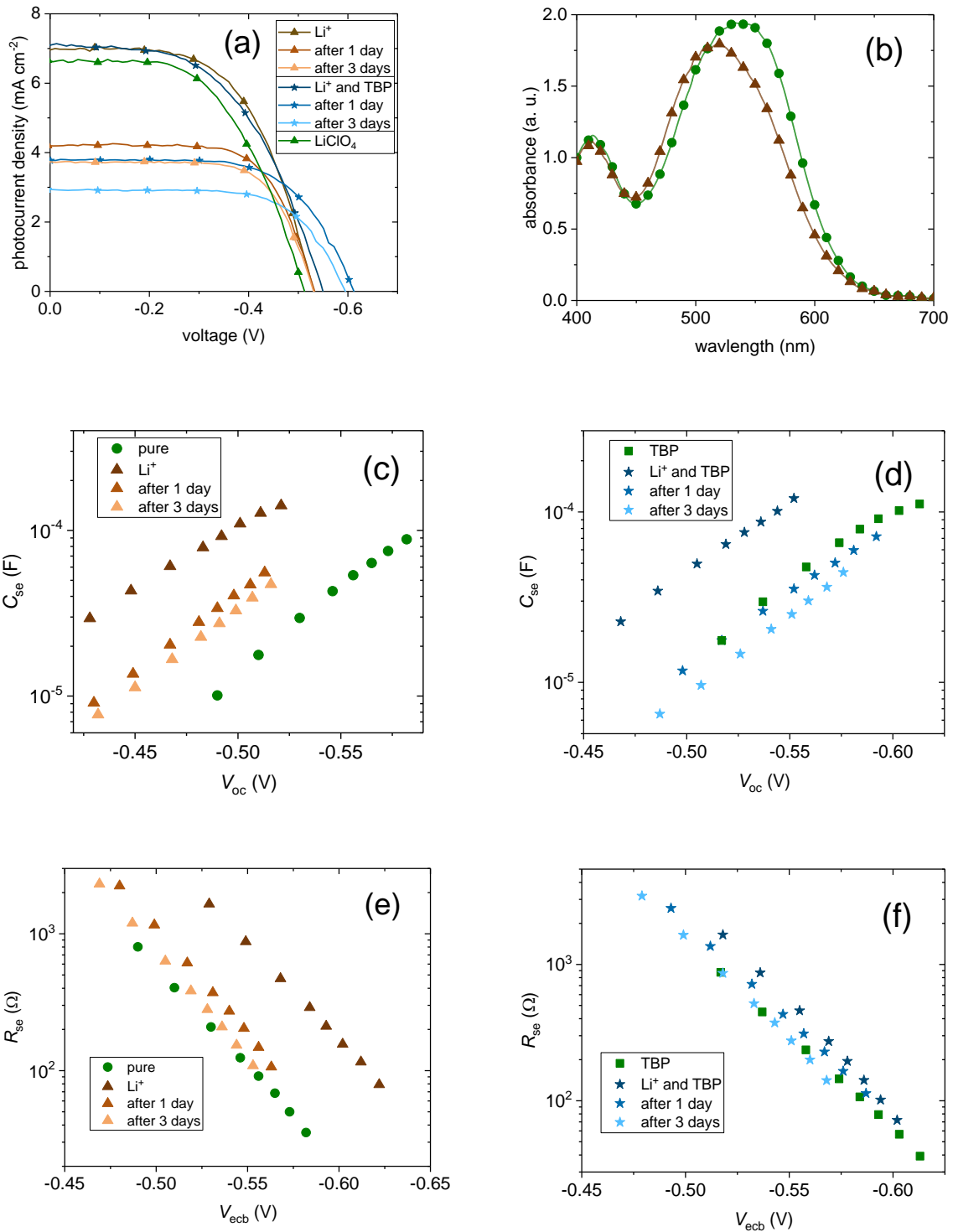


Figure S3. (a) I-V curves of ED-ZnO-based DSSCs with the temporal evolution in I-el containing Li⁺ or Li⁺ and TBP compared to I-el with Li⁺ ions from LiClO₄. (b) Diffuse transmission spectra of ED-ZnO-based cells with I-el either pure, (green) or with Li⁺ (brown). (c), (d) Temporal evolution of C_{se} and (e), (f) temporal evolution of R_{se} of the cells in (a).

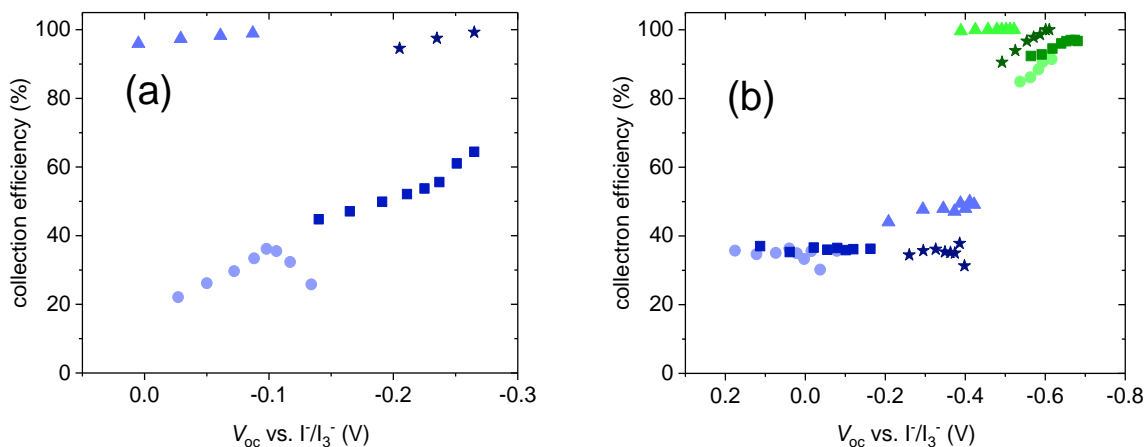


Figure S4. Charge collection efficiency of DSSCs determined from fitting the EIS data with different semiconductor and electrolyte compositions. (a) NP-TiO₂-based and (b) ED-ZnO-based DSSCs. The electrolyte composition is coded as in Figure S2. Transport in ED-ZnO-based cells with I-eI electrolytes occurred too fast to be detected in EIS indicating 100 % collection efficiency.

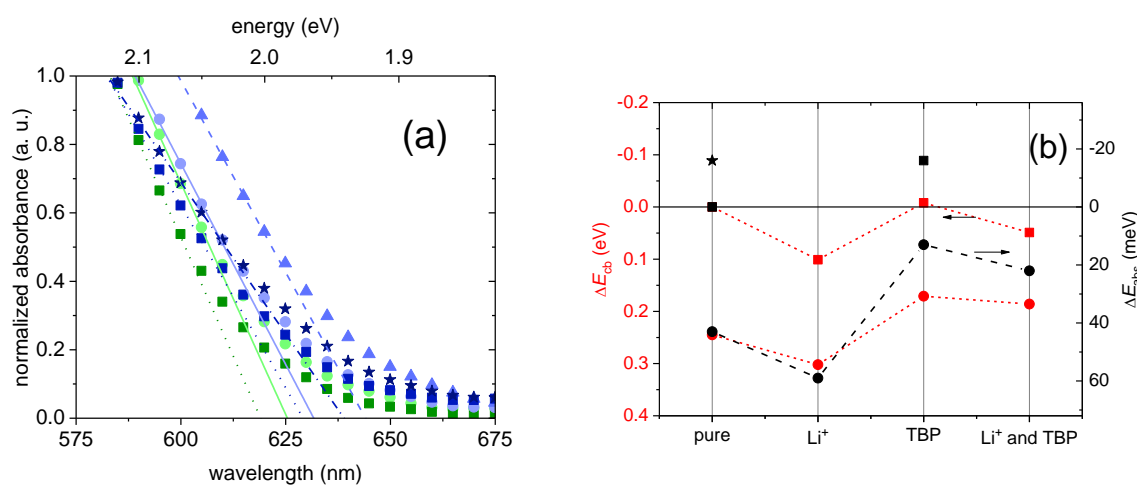


Figure S5. (a) Diffuse transmission spectra and linearly extrapolated absorption edge for ED-ZnO-based DSSCs with different electrolyte compositions coded as in Figure S2. (b) Relative conduction band edge shift ΔE_{cb} (red) from Figure 1e and relative absorption edge shift ΔE_{abs} (black) for ED-ZnO-based DSSCs with I-eI (squares) or Co-eI (circles). The relative absorption edge measured for a sensitized ED-ZnO photoanode in air is shown as a black star.

Evaluation of SECM data

A detailed description of the evaluation of SECM data is provided in refs.^{4,5}. The approach curves are fitted with the model of Cornut and Lefrou⁶ for finite irreversible kinetics at the sample yielding the dimensionless heterogeneous rate constant κ that is related to the effective rate constant k_{eff} (equation (SI-6)), in which r_T is the radius of the microdisk electrode and D the diffusion coefficient of the redox mediator determined from CVs and the $RG = r_{\text{glass}}/r_T$ values of 3.3 (I_3^-) and 4.36 ($[\text{Co}(\text{bpy-pz})_2]^{3+}$) from optical microscopy and r_T values.

$$\kappa = \frac{r_T k_{\text{eff}}}{D} \quad (\text{SI-6})$$

The curves in Figure S6 are plotted in normalized coordinates, i.e. the distance is given relative to r_T and the current is normalized to the steady-state diffusion-limited current $i_{T\infty}$ of the microelectrode in the solution bulk (at quasi infinite distance).

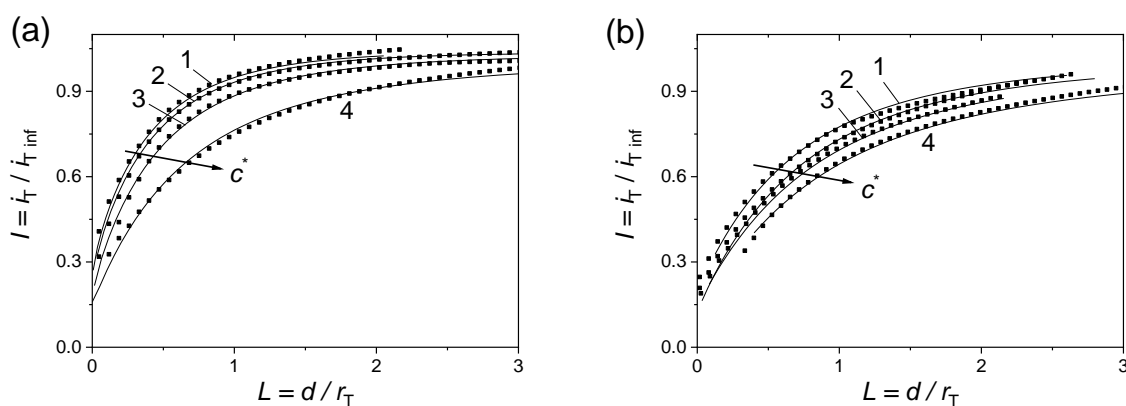


Figure S6. Microelectrode approach curves of the measured probe current i_T divided by the current measured at large distance $i_{T,\text{inf}}$ for sensitized ED-ZnO electrodes for (a) I_3^- for (a) bulk concentration c^* of I_3^- (1) 0.1 mM, (2) 0.2 mM, (3) 0.5 mM, (4) 1 mM; and (b) $[\text{Co}(\text{bpy-pz})_2]^{3+}$ (1) 0.2 mM, (2) 0.5 mM, (3) 1 mM, and (4) 2 mM.

In order to calculate the regeneration rate constant k_{ox} , the values for k_{eff} or k_{eff}^{-1} are fitted for different concentrations of oxidized redox mediator c^* according to equation (SI-7) for I_3^-/I^- ,⁴ or equation (SI-8) for $[\text{Co}(\text{bpy-pz})_2]^{3+/2+}$.⁵ Here, $\Gamma_D = 9.324 \cdot 10^{-7} \text{ mol cm}^{-2}$ is the dye loading (per geometric area) and $J_{\text{hv}} = 1.434 \cdot 10^{-5} \text{ mol cm}^{-2} \text{ s}^{-1}$ is the photon flux density.

$$\frac{1}{k_{\text{eff}}} = \frac{[I_3^-]^*}{J_{\text{hv}}} \frac{2}{\Gamma_D \Phi_{\text{hv}}} + \frac{2}{3\Gamma_D k_{\text{ox}}} \quad (\text{SI-7})$$

$$\frac{1}{k_{\text{eff}}} = \frac{[\text{Co}(\text{bpy}-\text{pz})_2^{3+}]^*}{J_{\text{hv}}} \frac{1}{\Gamma_D \Phi_{\text{hv}}} + \frac{1}{\Gamma_D k_{\text{ox}}} \quad (\text{SI-8})$$

Table S1. Heterogeneous rate constants κ and effective rate constants k_{eff} from fitting the approach curves in Figure S6 at different oxidized redox mediator concentrations.

	c^* (mM)	κ	k_{eff} ($10^{-3} \text{ cm s}^{-1}$)
I_3^-	0.1	0.277	2.03
	0.2	0.251	1.84
	0.5	0.184	1.35
	1	0.060	0.44
$[\text{Co}(\text{bpy}-\text{pz})_2^{3+}]$	0.2	0.077	0.18
	0.5	0.053	0.12
	1	0.026	0.06
	2	0.011	0.08

From the intercept b in Figure 4 of the main manuscript, one obtains k_{ox} for the two stoichiometries.

$$I_3^-/I^-: \quad k_{\text{ox}} = 2 b / (3 \Gamma_D)$$

$$[\text{Co}(\text{bpy}-\text{pz})_2]^{3+/2+}: \quad k_{\text{ox}} = b / (\Gamma_D)$$

This lead to the values summarized in Table S2. The I_3^-/I^- system is about one order of magnitude faster, which clearly exceeds the small difference between both models due to the different stoichiometry of both mediator systems.

Table S2: Fit results of k_{eff} from Table S2 shown in Figure 4

	b ($\mu\text{m s}^{-1}$)	k_{ox} ($\text{mol}^{-1} \text{ cm}^3 \text{ s}^{-1}$)
ED-ZnO, I-el	23.58	1686
ED-ZnO, Co-el	4.96	532

References

1. F. Fabregat-Santiago, G. Garcia-Belmonte, I. Mora-Seró and J. Bisquert, *Phys. Chem. Chem. Phys.*, 2011, **13**(20), 9083.
2. R. Ruess, S. Haas, A. Ringleb and D. Schlettwein, *Electrochim. Acta*, 2017, **258**, 591.
3. A. Hauch and A. Georg, *Electrochim. Acta*, 2001, **46**(22), 3457.
4. U. Mengesha Tefashe, K. Nonomura, N. Vlachopoulos, A. Hagfeldt and G. Wittstock, *J. Phys. Chem. C*, 2012, **116**(6), 4316.
5. H. Ellis, I. Schmidt, A. Hagfeldt, G. Wittstock and G. Boschloo, *J. Phys. Chem. C*, 2015, **119**(38), 21775.
6. R. Cornut and C. Lefrou, *J. Electroanal. Chem.*, 2008, **621**(2), 178.